

## Article

# Settlement Forecast of Marine Soft Soil Ground Improved with Prefabricated Vertical Drain-Assisted Staged Riprap Filling

Xue-Ting Wu <sup>1,2,\*</sup>, Jun-Ning Liu <sup>1</sup>, Adel Alowaisy <sup>2</sup>, Noriyuki Yasufuku <sup>2</sup>, Ryohei Ishikura <sup>2</sup> and Meilani Adriyati <sup>2</sup>

<sup>1</sup> Faculty of Engineering, China University of Geosciences, Wuhan 430074, China; liujunningljning@163.com

<sup>2</sup> Faculty of Engineering, Kyushu University, Fukuoka 8190395, Japan

\* Correspondence: wuxueting@cug.edu.cn

**Abstract:** By comparing different settlement forecast methods, eight methods were selected considering the creep of marine soft soils in this case study, including the Hyperbolic Method (HM), Exponential Curve Method (ECM), Pearl Growth Curve Modeling (PGCM), Gompertz Growth Curve Modeling (GGCM), Grey (1, 1) Model (GM), Grey Verhulst Model (GVM), Back Propagation of Artificial Neural Network (BPANN) with Levenberg–Marquardt Algorithm (BPLM), and BPANN with Gradient Descent of Momentum and Adaptive Learning Rate (BPGD). Taking Lingni Seawall soil ground improved with prefabricated vertical drain-assisted staged riprap filling as an example, forecasts of the short-term, medium-term, long-term, and final settlements at different locations of the soft ground were performed with the eight selected methods. The forecasting values were compared with each other and with the monitored data. When relative errors were between 0 and –1%, both the forecasting accuracy and engineering safety were appropriate and reliable. It was concluded that the appropriate forecast methods were different not only due to the time periods during the settlement process, but also the locations of soft ground. Among these methods, only BPGD was appropriate for all the time periods and locations, such as at the edge of the berm, and at the center of the berm and embankment.

**Keywords:** settlement forecast; marine soft soil ground; prefabricated vertical drain (PVD); staged riprap filling



**Citation:** Wu, X.-T.; Liu, J.-N.; Alowaisy, A.; Yasufuku, N.; Ishikura, R.; Adriyati, M. Settlement Forecast of Marine Soft Soil Ground Improved with Prefabricated Vertical Drain-Assisted Staged Riprap Filling. *Buildings* **2024**, *14*, 1316. <https://doi.org/10.3390/buildings14051316>

Academic Editors: Eugeniusz Koda and Harry Far

Received: 31 March 2024

Revised: 29 April 2024

Accepted: 3 May 2024

Published: 7 May 2024



**Copyright:** © 2024 by the authors. Licensee MDPI, Basel, Switzerland. This article is an open access article distributed under the terms and conditions of the Creative Commons Attribution (CC BY) license (<https://creativecommons.org/licenses/by/4.0/>).

## 1. Introduction

In coastal areas, the increase in population and economy induces a surge in land reclamation [1]. Construction in such low land areas comprised of soft soils is associated with serious post-construction settlement-related problems [2]. Therefore, settlement control is significant for the soft soil ground, and the ground settlement calculation and forecast play a vital role in all stages of engineering design, construction, and operation [3].

Terzaghi's consolidation theory (1923) [4] states that the consolidation time is proportional to the square of drainage distance. Several techniques were developed to reduce the consolidation time by shortening the drainage distance [5], such as the vertical drainage wells and utilization of Prefabricated Vertical Drain (PVD). PVD production consumes low energy, leading to fewer emissions and lower costs. Consequently, PVD is considered as an efficient and relatively cheap soft ground improvement technique [6].

Analytical calculation, numerical simulation, and prediction are commonly adopted in the engineering project design and construction for the settlement evaluation of soft soil ground. However, despite the extensive progress in PVD, several issues regarding the PVD design, installation, and performance are not well understood, including the smear zone dynamics [7], buckling and clogging of the PVD [8], and soil inhomogeneity, consequently leading to significant limitations in the existing consolidation and settlement evaluation theories [9]. For example, the layerwise summation method does not take into

account the lateral deformation [10], and the actual drainage performance of PVDs cannot be accurate when considered with existing analytical calculations during the consolidation and settlement over time.

In addition, numerical simulation has been widely employed as an alternative to avoid the analytical approaches of complex PVD-assisted preloading projects [11]. However, the prediction precision of numerical approaches is significantly affected by the material constitutive model and parameter selection. Furthermore, these methods are computationally intensive due to complicated boundary and loading conditions [2]. In particular, proper determination of the smear zone properties of PVDs is challenging [12]. Moreover, PVD is usually modeled as a solid element in a plane-strain state [13], resulting in significant computational difficulties and a remarkable difference in the soil-PVD configuration compared to the field [14]. Therefore, developing a reliable PVD model, considering the drainage consolidation effect without increasing the finite element nodes and excluding the plane-strain equivalent transformation, is greatly needed, but not completely solved yet.

In order to avoid the disadvantages associated with the analytical calculation and numerical simulation, the idea of settlement prediction based on the measured and monitored settlement data has been proposed [15]. Predictions and forecasts are simple and easy mathematical approaches, and have more accuracy as they fully consider the monitored data, which can reflect the real drainage effect of PVDs and the soil inhomogeneity. Moreover, settlement forecasts can be used for the real-time instruction of construction based on the real-time monitored data [16].

Most traditional settlement forecasts are based on the Empirical Formula Method (EFM), such as the Three-Point Method (3PM) [17], Asaoka Method (AM) [18], Hoshino Nori Method (HNM) [19], Hyperbolic Method (HM) [20], and Exponential Curve Method (ECM) [21], which are widely applied due to their simplicity [22]. Meanwhile, the Growth Curve Modeling (GCM) is referred to as a logistic curve with an S-shape having a similar pattern to the ground settlement [23]. It provides higher accuracy in forecasting settlement [24], such as Weibull Growth Curve Modeling (WGCM), Pearl Growth Curve Modeling (PGCM), and Gompertz Growth Curve Modeling (GGCM) [25].

Besides, Grey system theory is commonly used for sequence, topology, and system predictions [26]. The Grey (1, 1) Model (GM) is a basically and widely used Grey Prediction Model (GPM), especially for sequences with strong exponential regularity [27]. In addition, the Verhulst Model was aimed to limit the whole development for a real system and effectively describes a specific phenomenon, such as an S-shaped curve with a saturation region [28]. The newly combined utilization of Grey and Verhulst models, known as Grey Verhulst Model (GVM), was adopted in the deformation prediction [29].

Furthermore, Artificial Neural Network (ANN) is a powerful tool for tackling nonlinear problems and has been successfully adopted in optimizations [30], predictions, and forecasts [31]. Settlement is a complex nonlinear problem and is often difficult to express using an explicit mathematical expression [32]. Back Propagation (BP) is the most widely applied model in ANN [33]. For the BP of ANN (BPANN), in mathematics and computing, the Levenberg–Marquardt (LM) algorithm [34,35] is used to solve nonlinear least squares problems. Despite the advantages of BPANN, there are still some shortcomings associated with the traditional BPANN with LM algorithm (BPLM) [33], including: (i) it easily falls into local minimum rather than global optimum; (ii) it has a long training time and slow convergence speed for dealing with a huge amount of data; and (iii) the learning rate must be artificially selected before training. Thus, an improved BPANN with gradient descent of momentum and adaptive learning rate (BPGD) has been proposed [36].

The above methods are widely and successfully used in settlement predictions and forecasts for various types of soils in different engineering projects, such as in soft soils improved with vacuum-prefabricated vertical drain [37], foundation pit of artificial fill and silty clay layers [16], subgrade filled with construction and demolition waste [10], metro shield tunnel in saturated sand [38], and the full load-settlement curve of a strip footing [39]. Although the prediction or forecast accuracy has been significantly improved, there are

still errors between the predicted and observed magnitudes of settlements [40], which may be due to the application limitation and different suitability of each prediction or forecast method for varied situations and time periods. Consequently, it is particularly important to select the appropriate and reliable method according to the different soil properties and project characteristics.

Furthermore, especially, few studies considered settlement forecasting of deep marine soft soil ground improved with Prefabricated Vertical Drain (PVD)-assisted staged riprap filling technique [41], while studies comparing and optimizing the forecasting methods for such soft ground are lacking. Furthermore, there is no clear mechanism on the settlement of soft soil ground under this technology by reasons of the complexity of influencing factors during construction and limited engineering project data.

Therefore, in this study, by comparing the settlement forecast methods as summarized in Table 1 [42–45], the eight methods from four forecast types were selected considering the creep of soft soils, including HM, ECM, PGCM, GGCM, GM, GVM, BPLM, and BPGD, in which the GVM and BPGD were optimized from GM and BPLM, respectively. Taking Lingni Seawall constructed by PVD-assisted staged riprap filling as an example, forecasts of the short-term, medium-term, long-term, and final settlements at different locations of soft soil ground were performed. Moreover, the forecasting values were compared with each other and with the monitored data. In addition, relative errors and evaluation metrics in regression were analyzed for quantitatively studying the accuracy and reliability of various methods. Finally, the optimal methods of settlement forecasts in different locations and different time periods were studied to provide a reference for the selection of forecast methods for similar engineering projects, and to give a theoretical basis for practical engineering embankment settlement forecasts.

**Table 1.** Comparisons of different settlement forecast methods [42–45].

Forecast Method	Consideration of Creep	Requirement for Monitored Settlement Data
EFM	3PM	Constant load period, equidistant time series
	AM	
	HNM	Constant load period, any time series
	HM	
ECM	Yes	
GCM	WGCM	Whole or constant load period, equidistant time series
	PGCM	
	GGCM	
GPM	GM	Constant load period, equidistant time series
	GVM	Whole or constant load period, equidistant time series
BPANN	BPLM	Whole or constant load period, equidistant time series
	BPGD	

## 2. Methodology

In this study, taking Lingni Seawall constructed by PVD-assisted staged riprap filling as a case study, HM, ECM, PGCM, GGCM, GM, GVM, BPLM, and BPGD methods were adopted to analyze and forecast settlement processes and final settlements, as shown in Figure 1. It must be noted that for settlement monitoring data recorded at irregular intervals, a transformation to a regular interval is required when using GCM, GPM, and BPANN for forecasting [46]. Interpolation is commonly used to transform the unequal time interval settlement data; here, the cubic Spline method [47] was used to interpolate the recorded data.

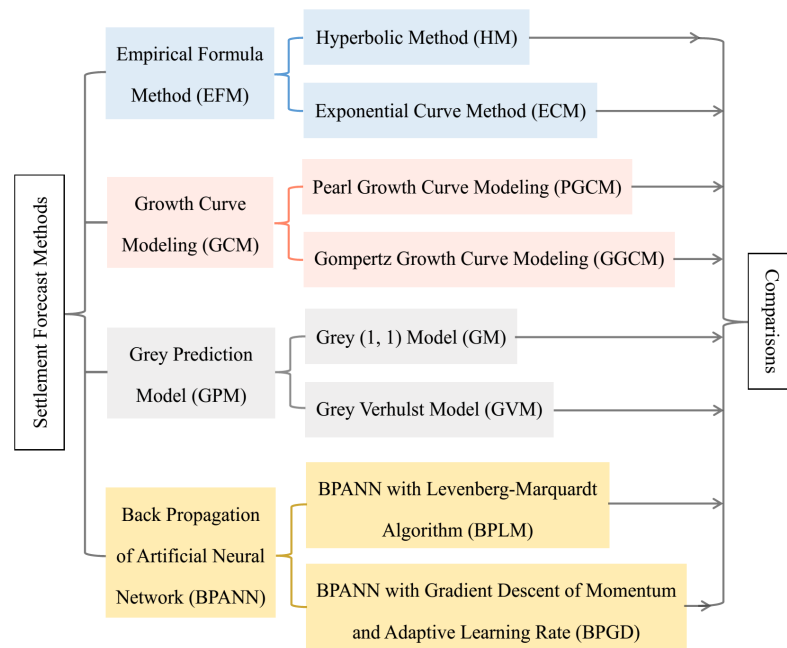


Figure 1. Forecast methods used in this study.

2.1. Case Study

2.1.1. Project Description

The Lingni Seawall project is located in Wenzhou, Zhejiang Province, China, as shown in Figure 2. Lingni Seawall is a stone embankment connecting Lingkun Island and Niyu Island. The embankment crest width is 10.5 m, with a crest elevation of 5.63 m in National Height Datum 1985 of China. The underlying ground exploration and boring data revealed that the soil profile was mainly comprised of marine muck with a thickness of about 30 m and mucky clay in deeper layer [48,49]. The combined PVD with the staged riprap preloading technique was adopted to improve the soft ground comprising the seawall foundation. The typical and representative foundation treatment and settlement monitoring cross-section of Lingni Seawall is shown in Figure 3.

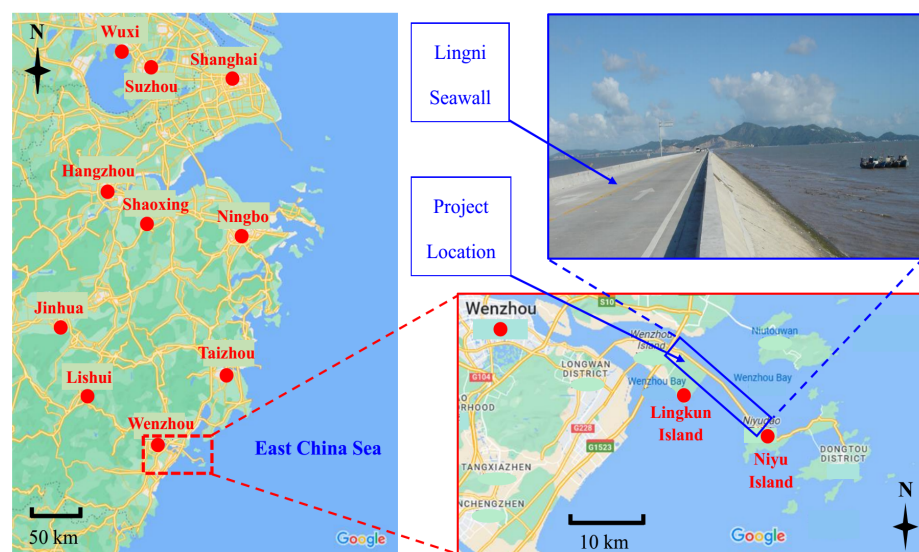
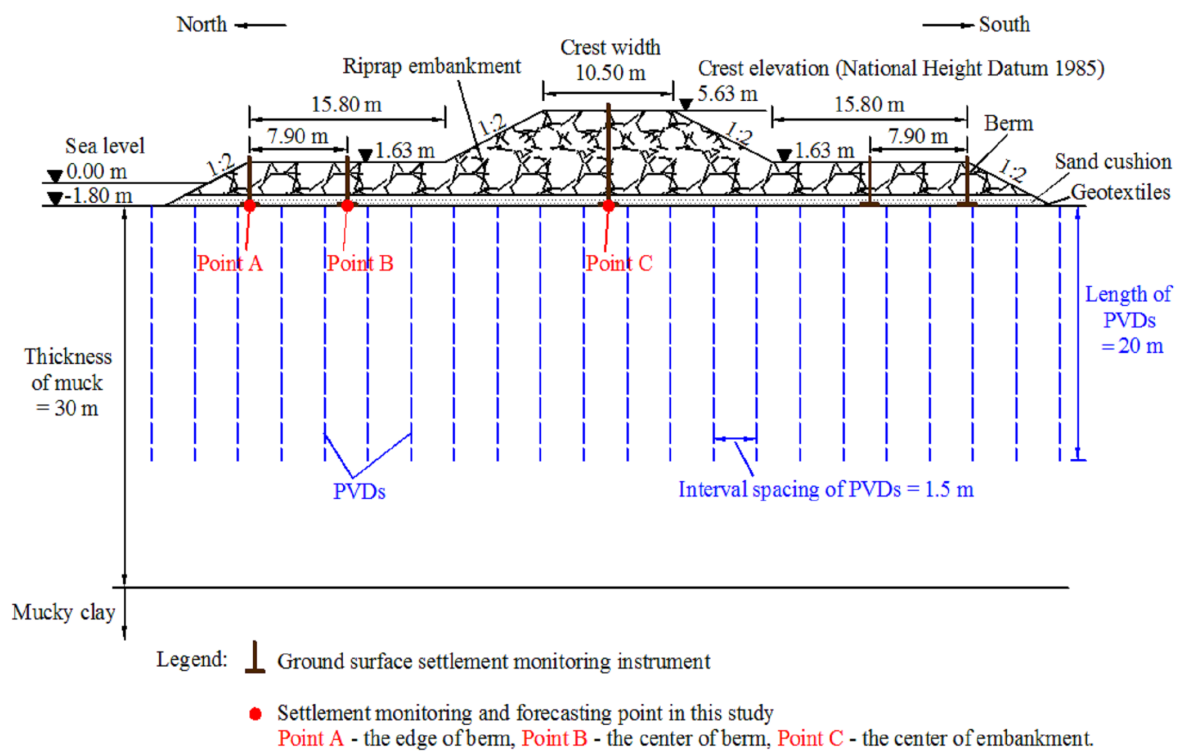


Figure 2. Geographic position of Lingni Seawall (Google Maps).



**Figure 3.** Typical foundation treatment and settlement monitoring cross-section of Lingni Seawall.

### 2.1.2. In Situ Settlement Monitoring

For controlling the riprap rate and monitoring the consolidation settlement regulation of Lingni Seawall, in situ monitoring and measurements of the ground surface settlements were performed. The positions of settlement measuring instruments are presented in Figure 3. Due to the symmetry of the embankment, Point A (the edge of the berm), Point B (the center of the berm), and Point C (the center of the embankment) were selected as the monitoring and forecasting points in this study.

The loading stages for various cross-sections or different parts of the same cross-section of the embankment were divided into different levels to reliably consider the difference construction conditions. For example, at Points A, B, and C of the representative foundation treatment cross-section, the riprap loading process (loading steps in kPa) was divided into 3, 3, and 7 stages, respectively. The monitored data of vertical ground surface settlements at Points A, B, and C are illustrated in Figure 4 and Table A1. We can see from Figure 4 that, in the first and second loading stages at Point C, the ground settlements at different points from large to small are as follows: Point A > Point B > Point C. However, with the loading increasing at the center of the embankment (after the third loading stage at Point C), the ground settlements from large to small become as follows: Point C > Point B > Point A. The reasons for these phenomena are mainly due to the inconsistency of the magnitude and time of loading at each point, the mutual influence between adjacent loadings and soils, and the heterogeneity of the ground soil distributions. Because of the complexity of ground settlement variability, it is difficult to use a unified formula or law to describe the settlements at different points of the soft ground. Therefore, in situ monitoring is a reliable method to accurately acquire the performance caused by loadings and PVDs [3], the settlement monitoring data was a comprehensive reflection of all the influencing factors on soft soil ground settlement in the processes of preloading, staged loading and constant loading. By forecasting the monitoring settlement data in advance, not only the staged riprap filling rate can be adjusted in time to guide the construction, but also the risk of excessive settlement can be forecasted in advance to avoid the occurrence of embankment instability.

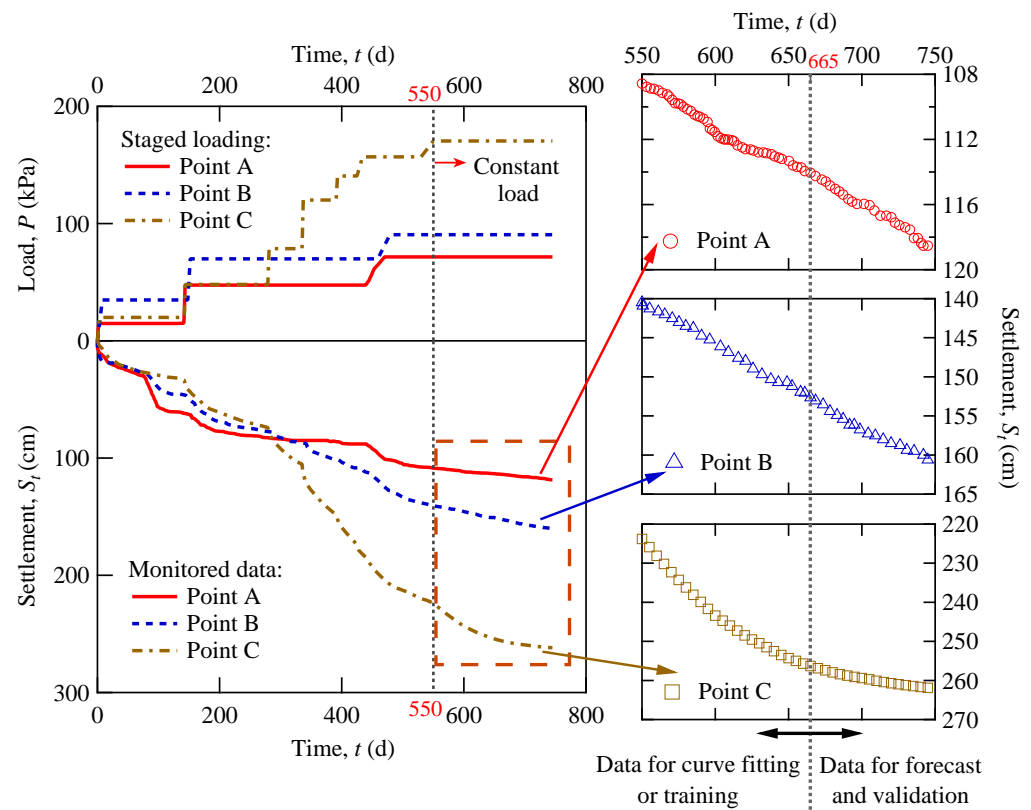


**Figure 4.** Staged riprap loading and monitored settlement data at Points A, B, and C. (Notes: 550 d—The full loading time at the center of the embankment, after which the loading will keep constant for the rest period; 665 d—The time of boundary point for settlement fitting and forecasting).

## 2.2. Empirical Formula Method (EFM)

The settlement forecast model can be established based on the measured settlement data, and the relationship between settlement and time for each measuring point will be obtained to forecast settlement variation [50]. Among all the settlement forecasting models, the empirical formula method (EFM) has the advantages of simple utilization and wide application range in engineering practices. Miyakawa (1961) [19] presented a settlement curve shape as a hyperbolic curve. Hoshino (1962) [19] modified the hyperbolic method with the proposal that settlement including shear strength is proportional to the square root of time. The previous studies have shown that the hyperbolic method (HM) gave very good forecasts of ultimate primary settlements for both laboratory oedometer tests and field settlements for clays with vertical drains [51,52]. In addition, the exponential curve method (ECM) has been shown to be reasonable and correct in the forecast of vertical ultimate bearing capacity of single pile [21] and the sure part of the roadbed settlement [53]. However, the applicability of these two most commonly used EFMs is worth discussing for the forecast of the PVD-assisted staged riprap filling foundation in deep marine soft soils.

### 2.2.1. Hyperbolic Method (HM)

The hyperbolic method assumes that the time dependence of settlement following a hyperbolic pattern as described in Equation (1) [20]:

$$S_t = S_0 + \frac{t - t_0}{a + b(t - t_0)} \quad (1)$$

where  $S_t$  is the settlement at the time  $t$ ;  $S_0$  is the settlement corresponding to the time  $t_0$ ;  $a$  and  $b$  are fitting parameters.

### 2.2.2. Exponential Curve Method (ECM)

The exponential curve describes the time dependence of settlement using an exponential formula as shown in Equation (2) [21]:

$$S_t = S_0 + a(1 - e^{-\frac{t-t_0}{b}}) \quad (2)$$

where  $S_t$ ,  $S_0$ ,  $t$ ,  $t_0$ ,  $a$ , and  $b$  hold the same meaning as in Equation (1).

### 2.3. Growth Curve Modeling (GCM)

Growth Curve Modeling (GCM) is widely used in fields such as ecology and demography. GCM is an S-shaped curve that reflects the process of a phenomenon happening, developing, maturing, and tending to saturation (limit) [23]. According to the theory of soil mechanics, the total ground settlement due to increased stresses can be divided into 3 parts: immediate settlement, primary consolidation settlement, and secondary compression settlement [54]. With the increase in load and time, the variation of foundation settlements can be divided into the following 4 stages: (1) The stage of the linear growth of the settlement. At the initial stage of loading, the soil is still in an elastic state. As the load increases, the settlement increases approximately linearly; (2) The stage of increasing settlement rate. As the load increases, the settlement and settlement rate of the soil ground increase continuously, showing obvious nonlinearity; (3) The stage of decreasing settlement rate. When the load no longer increases, due to the unfinished consolidation and the rheology of the soil, the ground settlement will continue to increase with the decreasing of the settlement rate; and (4) The stable stage of settlement. Theoretically, when the time tends to infinity, the ground settlement reaches the limit state of stability. From the above 4 stages of ground settlement process, we can see that it is very similar to the S-shaped development regulation described by GCM. Therefore, GCMs can be used to forecast the variation of ground settlement with time [55]. In this study, the commonly used Pearl Growth Curve Modeling (PGCM) and Gompertz Growth Curve Modeling (GGCM) were selected for the settlement forecasting of deep marine soft soils.

#### 2.3.1. Pearl Growth Curve Modeling (PGCM)

The Pearl curve is referred to as a logistic curve with an S-shape, which is named after the American biologist and demographer Raymond Pearl [23]. The Pearl curve can be expressed as shown in Equation (3) [23]:

$$S_t = \frac{a}{1 + be^{-ct}} \quad (3)$$

where  $t$  is the serial number of equidistant time series;  $S_t$  is the settlement at time serial number  $t$ ;  $a$ ,  $b$ , and  $c$  are fitting parameters.

#### 2.3.2. Gompertz Growth Curve Modeling (GGCM)

The Gompertz Growth Curve Modeling (GGCM) is a type of mathematical model for a time series, named after the British statistician and mathematician Benjamin Gompertz (1779–1865). It is a sigmoid function which describes growth as being slowest at the start and end of a given time period, as described in Equation (4) [25]:

$$S_t = ae^{-be^{-ct}} \quad (4)$$

where  $t$ ,  $S_t$ ,  $a$ ,  $b$ , and  $c$  hold the same meaning as in Equation (3).

### 2.4. Grey Prediction Model (GPM)

Grey system theory is an interdisciplinary scientific area that was first introduced by Deng (1982) [26]. The application fields of the Grey system involve agriculture, economy, geography, industry, geology, management, etc. Grey model based on Grey system theory can be used for comprehensive predictions in these various fields [56]. In different GPMs,

the Grey (1, 1) Model (GM) is especially used for sequences with strong exponential regularity [27]. Therefore, the GM is similar to the ECM among the aforementioned empirical formula method. Based on this, the GM was adopted in this study for the settlement forecasting and method comparison research, due to its different data processing methods compared to the ECM.

In addition, for completely eliminating the inherent simulant error and avoiding the jumping errors from the differential equation to differential equation in traditional Grey modeling, the Grey Verhulst Model (GVM) was adopted in this study. The GVM is a newly combined utilization of Grey and Verhulst models, of which the Verhulst model was first introduced by the German biologist Pierre Franois Verhulst. Previous case analysis showed that the simulation and forecasting accuracy in traditional modeling has been significantly improved by GVM [57].

#### 2.4.1. Grey (1, 1) Model (GM)

For the Grey (1, 1) Model (GM), after the interpolation [47], it is assumed that the settlement increment sequence in the equal time interval is the original sequence ( $S^{(0)}$ ), as shown in Equation (5) [56]:

$$S^{(0)} = \{S^{(0)}(1), S^{(0)}(2), \dots, S^{(0)}(n)\} \quad (5)$$

Then, the first-order accumulated generating operation sequence (1-AGO sequence,  $S^{(1)}$ ) can be generated from  $S^{(0)}$  following Equation (6):

$$\begin{cases} S^{(1)} = \{S^{(1)}(1), S^{(1)}(2), \dots, S^{(1)}(n)\} \\ S^{(1)}(t) = \sum_{i=1}^t S^{(0)}(i), t = 1, 2, \dots, n \end{cases} \quad (6)$$

The mean-generating sequence ( $Z^{(1)}$ ) of  $S^{(1)}$  can be calculated by Equation (7):

$$\begin{cases} Z^{(1)} = \{Z^{(1)}(2), Z^{(1)}(3), \dots, Z^{(1)}(n)\} \\ Z^{(1)}(t) = 0.5S^{(1)}(t) + 0.5S^{(1)}(t-1), t = 2, 3, \dots, n \end{cases} \quad (7)$$

From Equations (6) and (7), the differential equation of GM can be described as in Equation (8):

$$S^{(0)}(t) + aZ^{(1)}(t) = b \quad (8)$$

where— $a$  is the development coefficient;  $b$  is the grey action quantity.

After solving the GM function of Equation (8), the time response ( $\hat{S}^{(1)}(k)$ ) of GM, here refers to the predicted settlement, can be expressed by Equation (9) as follows:

$$\hat{S}^{(1)}(t) = (S^{(0)}(1) - \frac{b}{a})e^{-at} + \frac{b}{a}, t = 1, 2, \dots, n \quad (9)$$

#### 2.4.2. Grey Verhulst Model (GVM)

The difference from GM is that the GVM has a different and more complex differential equation as expressed in Equation (10) [28]:

$$S^{(0)}(t) + aZ^{(1)}(t) = b(Z^{(1)}(t))^2 \quad (10)$$

where— $a$  and  $b$  hold the same meaning as in Equation (8).

After solving the GVM function of Equation (10), the time response ( $\hat{S}^{(1)}(k)$ ) of GVM, here also referring to the predicted settlement, can be expressed by Equation (11) [57] as follows:

$$\hat{S}^{(1)}(t) = \frac{aS^{(0)}(1)}{bS^{(0)}(1) + [a - bS^{(0)}(1)]e^{a(t-1)}}, t = 1, 2, \dots, n \quad (11)$$

## 2.5. Back Propagation of Artificial Neural Network (BPANN)

Ever since nonlinear functions that work recursively (i.e., artificial neural networks) were introduced to the world of machine learning, its applications have been booming. In this context, the proper training of a neural network is the most important aspect of making a reliable model. Back propagation is the neural network training process of feeding error rates back through a neural network to make it more accurate. Although effectiveness of Back Propagation of Artificial Neural Network (BPANN) is visible in most real-world deep learning applications [31], it is never examined in the case of the settlement forecasting of the PVD-assisted staged riprap filling foundation in deep marine soft soils. Therefore, in this study, two kinds of BPANN were selected for forecasts of the short-term, medium-term, long-term, and final settlements at different locations of the soft soil ground.

### 2.5.1. BPANN with Levenberg–Marquardt Algorithm (BPLM)

BPANN generally has a multi-layer structure, the simplest of which is a three-layer perceptron network [33], as shown in Figure 5.

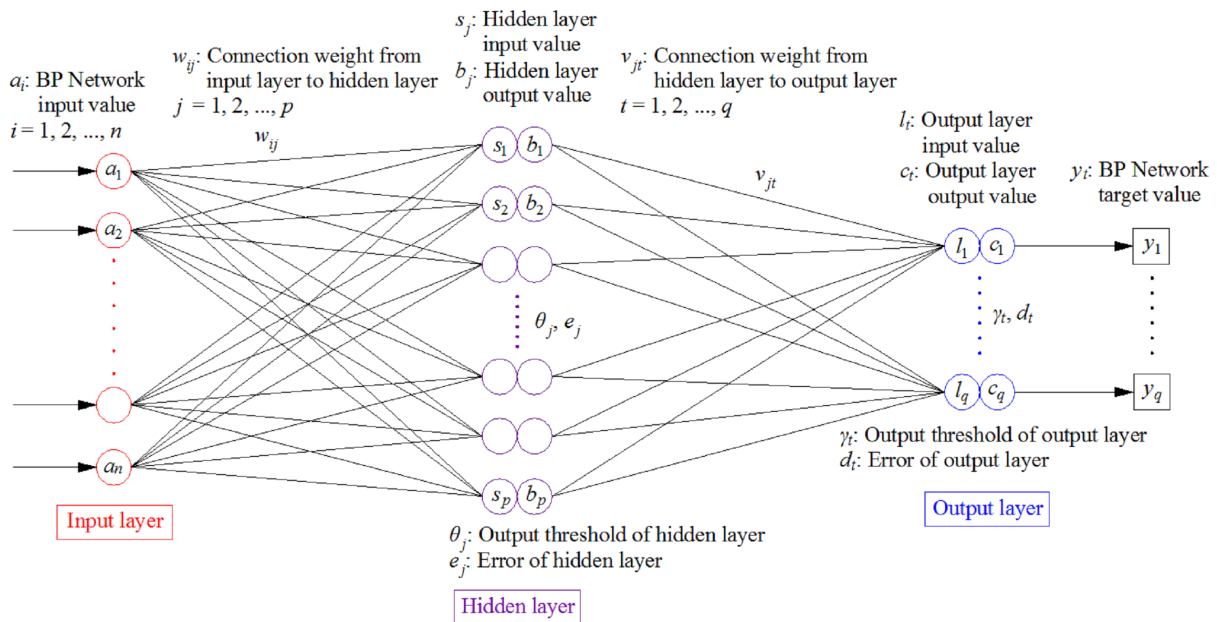


**Figure 5.** Three-layer perceptron network of BPANN.

The mathematical model of the three-layer perceptron of BPANN is described in Equation (12) for a hidden layer, while Equation (13) describes the output layer with the symbols annotated in Figure 5. In Equations (12) and (13),  $f(x)$  is a unipolar or bipolar Sigmoid function, which is a nonlinear transfer function as shown in Equation (14) [33].

$$\begin{cases} s_j = \sum_{i=1}^n w_{ij} a_i - \theta_j \\ b_j = f(s_j) \end{cases} \quad (12)$$

$$\begin{cases} l_t = \sum_{j=1}^p v_{jt} b_j - \gamma_t \\ c_t = f(l_t) \end{cases} \quad (13)$$

$$f(x) = \frac{1}{1 + e^{-x}} (\text{Unipolarity}); f(x) = \frac{1 - e^{-x}}{1 + e^{-x}} (\text{Bipolarity}) \quad (14)$$

Furthermore, in this study, the BPANN was produced using MATLAB (Ver. 9.8, MathWorks, USA), and the most commonly used LM algorithm [34,35] was adopted for solving generic curve-fitting problems.

### 2.5.2. BPANN with Gradient Descent of Momentum and Adaptive Learning Rate (BPGD)

In order to avoid the shortcomings associated with the BPLM [33], an improved BPANN with gradient descent of momentum and adaptive learning rate (BPGD) [36] was used in this study for the settlement forecasting and method comparison research. Instead of LM algorithm, the additional momentum method in Equation (15) and the self-adaptive learning rate method in Equation (16) are adopted in BPGD, respectively.

$$\begin{cases} w_{ij}(k+1) = (1 - m_c)\eta e_j a_i + m_c w_{ij}(k) \\ \theta_j(k+1) = (1 - m_c)\eta e_j + m_c \theta_j(k) \end{cases} \quad (15)$$

where  $k$  is the training epoch;  $m_c$  is the momentum coefficient, and  $m_c \in (0, 1)$ ;  $\eta$  is the learning rate; other symbols are annotated in Figure 5. Using Equation (15), it can effectively avoid  $w_{ij} = 0$ , and thus makes the network jump off from a local minimum of the error.

$$\eta(k+1) = \begin{cases} 1.05\eta(k), & E(k+1) < E(k) \\ 0.7\eta(k), & E(k+1) > 1.04E(k) \\ \eta(k), & E(k) \leq E(k+1) \leq 1.04E(k) \end{cases} \quad (16)$$

where  $E$  is the square error function, which represents the mean-squared error between actual outputs and target outputs of the network; other symbols are the same to Equation (15).

## 3. Results

### 3.1. Curve Fitting and Training Results

Based on load-settlement-time monitored data at Points A, B, and C illustrated in Figure 4, after 550 days of staged loading, the marine soil profile's full loading was achieved and remained constant for the rest period. Therefore, the 550-day settlement and time were selected as the initial settlement ( $S_0 = 108.57$  cm for Point A; 140.48 cm for Point B; and 223.80 cm for Point C) and initial time ( $t_0 = 550$  d for Points A, B, and C). After achieving the constant load, field monitoring was carried out for 195 days. Taking the monitored data between day 550 and day 665 for curve fittings (EFMs, GCMs, and GPMs) or trainings (BPANNs), the monitored data between day 665 and day 745 were used for forecasts and validations, as indicated in Figure 4. Furthermore, for GCMs, GPMs, and BPANNs, the cubic Spline method with a 5-day regular time interval during the constant load period was applied to interpolate the recorded data for Points A, B, and C.

For BPANNs, meanwhile, due to the lack of explicit mathematical expression, an algorithm program using MATLAB was adopted. In BPANNs, every four adjacent consecutive settlements with equal time interval ( $\Delta t = 5$  d) were taken as an input sample sequence ( $a_1, a_2, a_3$ , and  $a_4$ ), and the immediately adjacent fifth settlement was considered as the target sample ( $y_1$ ), as shown in Figure 5. In this study, the number of input layer units for each set of training samples is  $n = 4$ , the number of output layer units is  $q = 1$ , and the formula for determining the number of hidden layer units  $p$  can be calculated by Equation (17) [58]:

$$p = \sqrt{n+q} + x \quad (17)$$

where  $p$ ,  $n$ , and  $q$  are annotated in Figure 5. And parameter  $x \in (1, 10)$  [58], thus  $p \in (3, 12)$ , and the optimal value of  $p$  can be judged by the BPANN training error.

Taking Point B as an example, when  $p = 8$ , the neural network and weight matrices (**W**) of BPLM and BPGD are presented in Figure 6.

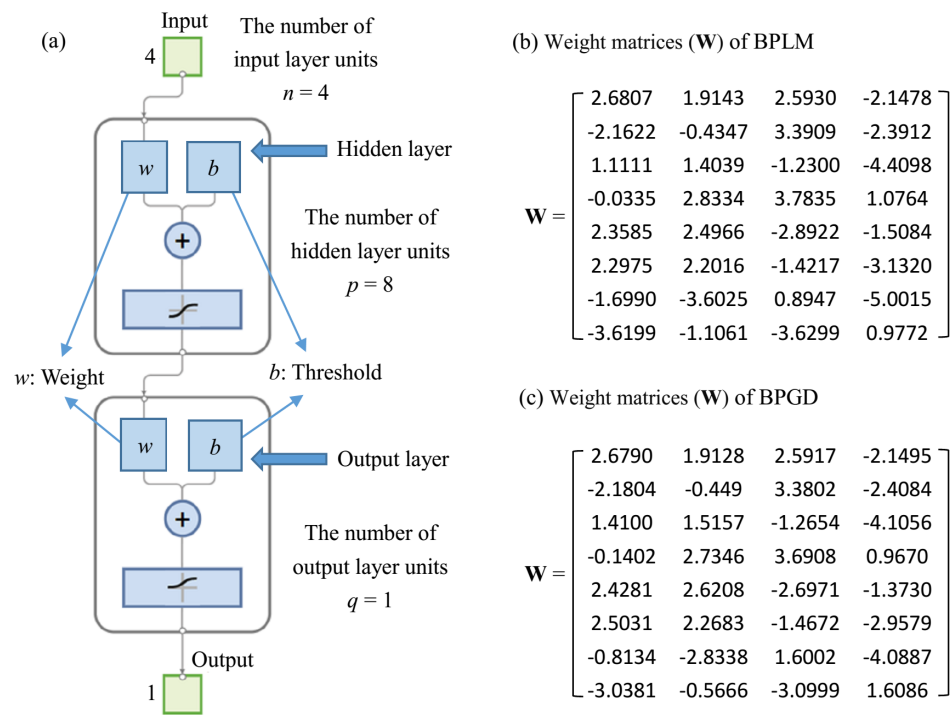


**Figure 6.** BPANN at Point B: (a) neural network of BPLM and BPGD; (b) weight matrices of BPLM; (c) weight matrices of BPGD.

The curve fitting and training results based on the settlement-time period between day 550 and 665 at Points A, B, and C are illustrated in Figures 7, 8 and 9, respectively. It can be seen that all the fitting and training results of the eight methods were in good agreement with the monitored data. Therefore, we can use these fitting and training results for subsequent settlement forecasting.

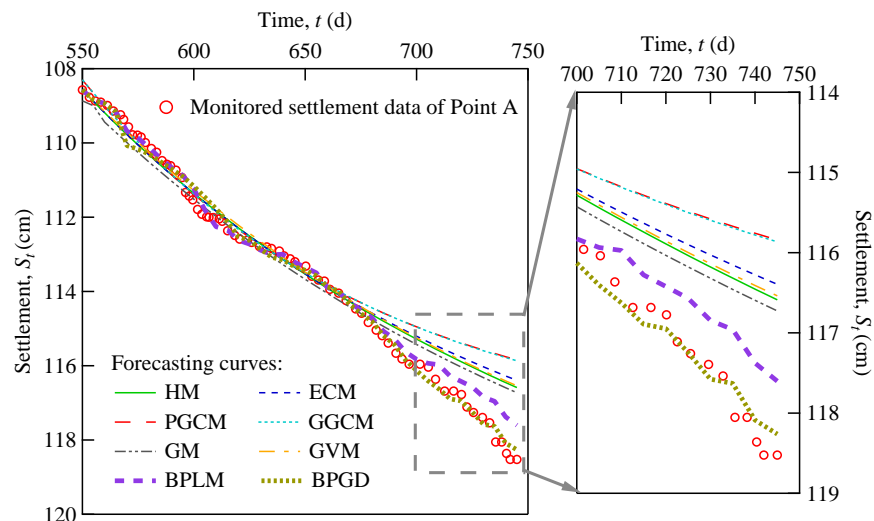


**Figure 7.** Monitored data and settlement fitting and forecasting results of Point A.

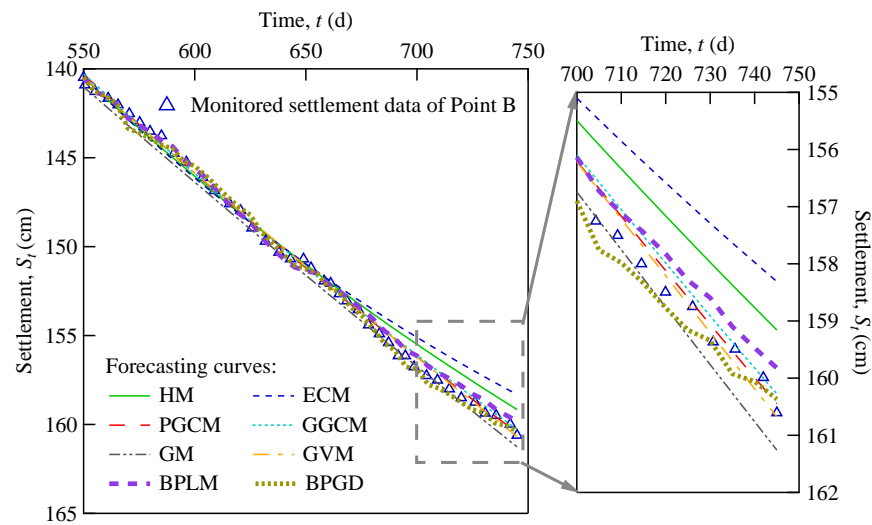


Figure 8. Monitored data and settlement fitting and forecasting results of Point B.

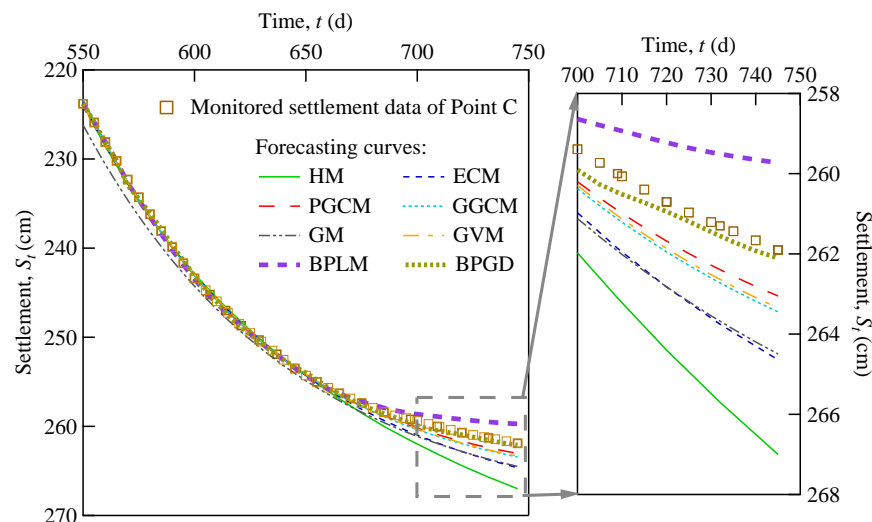


Figure 9. Monitored data and settlement fitting and forecasting results of Point C.

### 3.2. Comparison of Settlement Forecast Results

Through curve fittings by HM, ECM, PGCM, GGCM, GM, and GVM, the settlement forecasting formulas were obtained as expressed in Equations (18)–(23), respectively. In Equations (18) and (19),  $t$  is the real time with the unit of day. However, in Equations (20)–(23),  $t$  refers to the serial number of equidistant time series,  $t = 1, 2, \dots, n$ . Then, forecasts of the settlement-time period between day 665 and 745 at Points A, B, and C were performed. The eight settlement forecasting curves and in situ monitored data of the typical cross-section at Points A, B, and C are presented in Figures 7, 8 and 9, respectively.

$$HM : \begin{cases} S_t = 108.57 + \frac{t - 550}{15.76 + 0.044 \times (t - 550)} & (PointA) \\ S_t = 140.48 + \frac{t - 550}{8.49 + 0.010 \times (t - 550)} & (PointB) \\ S_t = 223.80 + \frac{t - 550}{1.96 + 0.013 \times (t - 550)} & (PointC) \end{cases} \quad (18)$$

$$ECM : \begin{cases} S_t = 108.57 + 12.45 \times (1 - e^{-\frac{t-550}{197.03}}) & (PointA) \\ S_t = 140.48 + 39.12 \times (1 - e^{-\frac{t-550}{320.49}}) & (PointB) \\ S_t = 223.80 + 46.87 \times (1 - e^{-\frac{t-550}{95.13}}) & (PointC) \end{cases} \quad (19)$$

$$PGCM : \begin{cases} S_t = \frac{117.84}{1 + 0.092e^{-0.042t}} & (PointA) \\ S_t = \frac{207.94}{1 + 0.49e^{-0.013t}} & (PointB) \\ S_t = \frac{266.39}{1 + 0.21e^{-0.070t}} & (PointC) \end{cases} \quad (20)$$

$$GGCM : \begin{cases} S_t = 118.03e^{-0.090e^{-0.039t}} & (PointA) \\ S_t = 213.54e^{-0.42e^{-0.0098t}} & (PointB) \\ S_t = 267.50e^{-0.19e^{-0.063t}} & (PointC) \end{cases} \quad (21)$$

$$GM : \begin{cases} \hat{S}^{(1)}(t) = -11.91e^{-0.021t} + 120.48 & (PointA) \\ \hat{S}^{(1)}(t) = -245.88e^{-0.0022t} + 386.36 & (PointB) \\ \hat{S}^{(1)}(t) = -47.14e^{-0.053t} + 270.94 & (PointC) \end{cases} \quad (22)$$

$$GVM : \begin{cases} \hat{S}^{(1)}(t) = \frac{2.71}{0.023 + 0.0022e^{-0.025 \times (t-1)}} & (PointA) \\ \hat{S}^{(1)}(t) = \frac{1.35}{0.0058 + 0.0038e^{-0.0096 \times (t-1)}} & (PointB) \\ \hat{S}^{(1)}(t) = \frac{14.77}{0.056 + 0.010e^{-0.066 \times (t-1)}} & (PointC) \end{cases} \quad (23)$$

From Figure 7, it was found that all the forecasting settlement values were smaller than the monitored data except the BPGD. This demonstrates that the other seven forecasting results were unsafe for soft soil foundation at the edge of the berm (Point A). This might be due to the fact that the settlement at Point A was not only controlled by the staged loading of the berm, but also largely affected by the later staged loading of the embankment. This phenomenon can also be observed from the monitored curves at Point A in Figure 4.

For the settlement forecasting at the center of the berm (Point B), the results of five methods were relatively close to the monitored data, including PGCM, GGCM, GM, GVM, and BPGD, as illustrated in Figure 8. But for HM, ECM, and BPLM, the forecasting settlement values were unsafe for soft soil foundation here, since they were smaller than the monitored values.

The settlement forecasting at the center of the embankment (Point C) had a completely different result to Point A. It was found from Figure 9 that all the forecasting settlement values were larger than the monitored data except the BPLM. From the perspective of the forecasting method itself, this may be due to the fact that the BPLM has the shortcoming associated with falling into local minimum. From an engineering point of view, this might be due to the fact that the settlement at Point C was only controlled by the staged loading at the center of the embankment. It can be observed from the monitored curves of Point C in Figure 4 that the settlements were highly consistent with the staged loading variation patterns. Therefore, under the influence of this single factor, the other forecasting settlement values were generally greater than the monitored data at the center of the embankment.

The above results suggested that, settlement forecasting always overestimated the settlement at the center of the embankment and underestimated the settlement at the edge of the berm. However, between these two locations at the center of the berm, more settlement forecasts were appropriate mainly due to the combination of various factors

on its settlement, such as the load increasing at the center of the embankment and the constrained deformations in the horizontal direction.

### 3.3. Error Analysis

For quantitatively studying the accuracy and reliability of various settlement forecast methods to control the staged riprap filling rate and evaluate the consolidation effectiveness of deep marine soft soil foundations, the relative errors ( $e = (\text{measured value} - \text{predicted value}) / \text{measured value}$ , %) of various forecast methods were calculated as presented in Figure 10. Furthermore, the maximum values of positive and negative relative errors and the mean values of positive and negative relative errors are listed in Table 2.

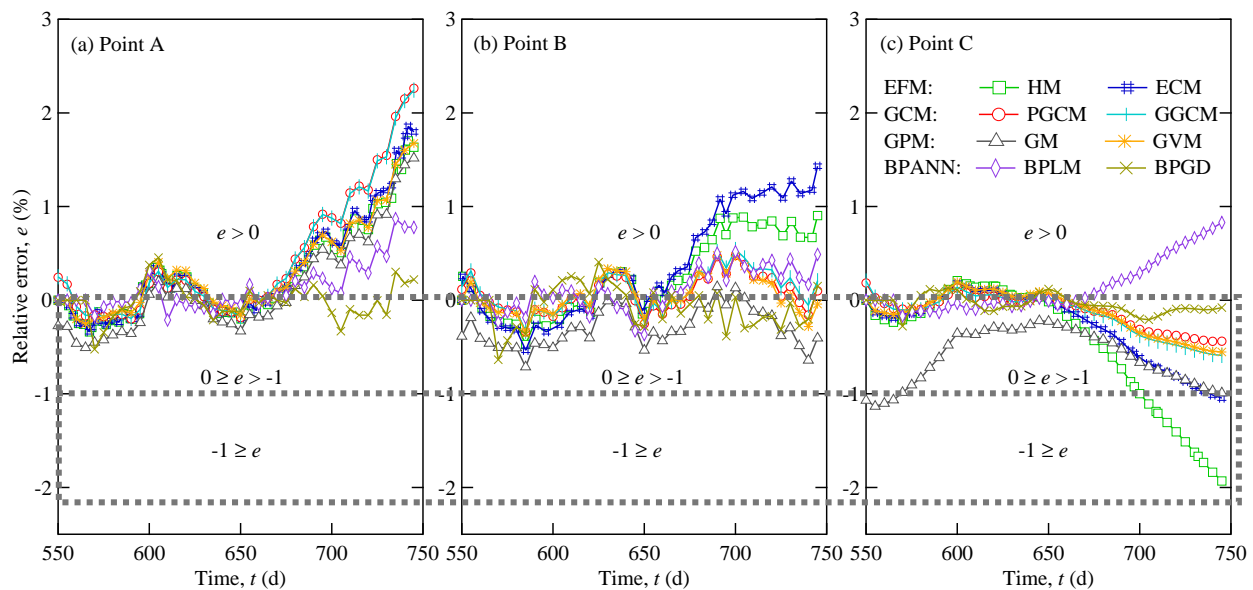


**Figure 10.** Comparison of relative errors of different forecast methods: (a) error analysis of Point A, (b) error analysis of Point B, (c) error analysis of Point C.

Based on the two principles of forecasting accuracy and engineering safety, scilicet, (i) the smaller the relative error, the higher the prediction accuracy, and (ii) when the relative error is negative, the higher the safety of the forecasting than a positive relative error. Thus, forecast methods can be evaluated by relative errors following Figure 10. Generally speaking, when  $0 \geq e > -1\%$ , both the forecasting accuracy and engineering safety are appropriate and reliable. Therefore, for settlement forecast at the edge of the berm (Point A), only BPGD was available. Additionally, PGCM, GGCM, GM, GVM, and BPGD were available for settlement forecast at the center of the berm (Point B). In addition, for settlement forecast at the center of the embankment (Point C), PGCM, GGCM, GVM, and BPGD were available. Among these eight forecast methods, only BPGD was appropriate and reliable for all Points A, B, and C.

**Table 2.** Relative error analysis of different forecast methods.

Forecast Method	Point	Relative Error, $e$ (%)			
		Maximum Value		Mean Value	
		Positive	Negative	Positive	Negative
HM	A	1.701	−0.338	0.544	−0.160
	B	0.903	−0.474	0.514	−0.185
	C	0.208	−1.932	0.100	−0.606

Table 2. Cont.

Forecast Method	Point	Relative Error, $e$ (%)			
		Maximum Value		Mean Value	
		Positive	Negative	Positive	Negative
ECM	A	1.857	−0.338	0.580	−0.164
	B	1.430	−0.535	0.687	−0.241
	C	0.180	−1.046	0.072	−0.368
PGCM	A	2.263	−0.201	0.692	−0.143
	B	0.476	−0.340	0.209	−0.112
	C	0.184	−0.439	0.060	−0.189
GGCM	A	2.243	−0.180	0.691	−0.138
	B	0.541	−0.333	0.240	−0.102
	C	0.204	−0.589	0.066	−0.243
GM	A	1.516	−0.507	0.570	−0.257
	B	0.142	−0.713	0.099	−0.326
	C	0	−1.135	0	−0.606
GVM	A	1.675	−0.253	0.606	−0.107
	B	0.478	−0.282	0.222	−0.110
	C	0.194	−0.554	0.089	−0.256
BPLM	A	0.871	−0.212	0.248	−0.075
	B	0.518	−0.368	0.241	−0.155
	C	0.829	−0.169	0.390	−0.070
BPGD	A	0.455	−0.524	0.154	−0.154
	B	0.406	−0.636	0.140	−0.250
	C	0.129	−0.278	0.081	−0.099

### 3.4. Evaluation Metrics Analysis in Regression

To further evaluate the accuracy of these forecasting models, the sum of squares due to error (SSE), mean squared error (MSE), root mean squared error (RMSE), mean absolute error (MAE), and coefficient of determination or R-squared ( $R^2$ ) were used to evaluate the performance of each model in regression analysis. The evaluation metrics analysis of eight forecast methods at Points A, B, and C are presented in Table 3.

**Table 3.** Evaluation metrics analysis of different forecast methods. (SSE—Sum of squares due to error; MSE—Mean squared error; RMSE—Root mean squared error; MAE—Mean absolute error;  $R^2$ —R-squared).

Forecast Method	Point	SSE	MSE	RMSE	MAE	$R^2$
HM	A	31.453	0.437	0.661	0.443	0.943
	B	24.069	0.602	0.776	0.616	0.984
	C	79.462	3.179	1.783	1.084	0.975
ECM	A	37.887	0.526	0.725	0.477	0.932
	B	47.840	1.196	1.094	0.841	0.967
	C	26.433	1.057	1.028	0.665	0.992
PGCM	A	36.502	0.913	0.955	0.612	0.886
	B	3.942	0.099	0.314	0.251	0.997
	C	12.066	0.302	0.549	0.393	0.998
GGCM	A	35.972	0.899	0.948	0.609	0.888
	B	5.139	0.129	0.358	0.282	0.997
	C	19.461	0.487	0.698	0.486	0.996

Table 3. Cont.

Forecast Method	Point	SSE	MSE	RMSE	MAE	R <sup>2</sup>
GM	A	16.054	0.401	0.634	0.462	0.950
	B	11.523	0.288	0.537	0.462	0.992
	C	109.871	2.747	1.657	1.503	0.978
GVM	A	19.706	0.493	0.702	0.468	0.939
	B	4.040	0.101	0.318	0.248	0.997
	C	17.501	0.438	0.662	0.488	0.997
BPLM	A	4.757	0.132	0.364	0.242	0.979
	B	5.902	0.164	0.405	0.331	0.995
	C	26.326	0.731	0.855	0.569	0.990
BPGD	A	1.813	0.050	0.224	0.175	0.992
	B	4.707	0.131	0.362	0.303	0.996
	C	2.701	0.075	0.274	0.238	0.999

The smaller the value of SSE, the better the model. Table 3 shows that, the BPGD was the best forecast model with the smallest SSE and the highest R<sup>2</sup> among these eight methods. However, for settlement forecasting, even the BPLM had a smaller SSE and a higher R<sup>2</sup>, but the BPLM was not safe for its smaller forecasting value than the measured value. Therefore, both evaluation metrics analysis and error analysis need to be considered when selecting settlement forecasting models.

Furthermore, the above conclusions were only based on the comparison with the monitored data from 665 to 745 days. According to the previous studies [59–61], the period of settlement forecast can be divided into the short-term (less than about 550 days), medium-term (less than about 750 days) and long-term (more than about 750 days). Therefore, the above conclusions were suitable and reliable for the short-term and medium-term settlement forecasting, but for long-term and final settlement (time approaching infinity) forecasting, further research and verification should be carried out.

### 3.5. Final Settlement Forecast

When time approached infinity, the final settlement can be calculated following Equations (18)–(23) for EFMs, GCMs, and GPMs, respectively. Since BPANNs are based on the input set to obtain the target set, they are unable to find limits at time infinity by using mathematical expressions like other methods. However, according to the design service life of the embankment (20 years), its final settlement value at that time can be forecasted by BPANNs. Thus, all the forecasted final settlements ( $S_{\infty}$ ) are presented in Figure 11.

Due to the lack of monitored data of the final settlement, the applicability of forecast methods can be inferred only based on the current normal operation of the Lingni Seawall embankment. Therefore, HM was inappropriate for Points A, B, and C for the too-large forecasting values. For the same reason, GM for Point B was also inappropriate for forecasting. Additionally, BPLM was inappropriate for Points A, B, and C, because the forecasted final settlements were close to or less than the 745-day monitored data, which will lead to the lack of safety of engineering project. For this reason, PGCM and GGCM were not reliable for Point A.

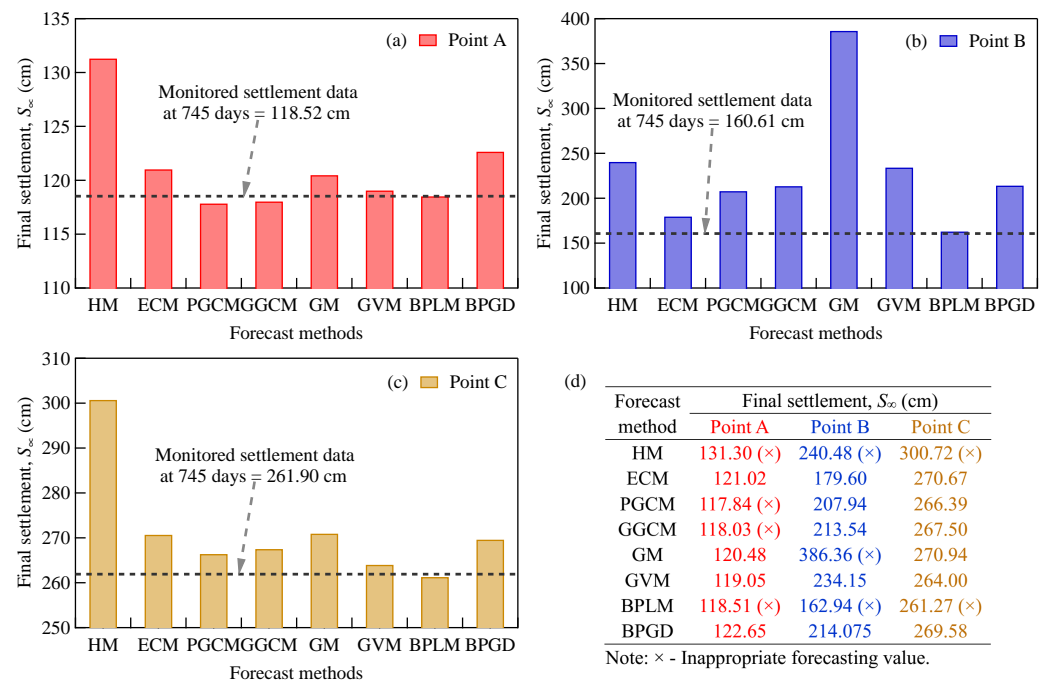


Figure 11. Comparison of final settlement forecasts: (a) forecasts at Point A, (b) forecasts at Point B, (c) forecasts at Point C, (d) forecasted final settlement values.

#### 4. Discussion

From the above settlement fitting or training results as shown in Figures 7–9, we can find that all the fitting and training results of the eight methods were in good agreement with the monitored data. However, for different time periods in the settlement process and different locations of marine soft soil foundation under embankment construction for this case study, the appropriate and reliable settlement forecast methods were different. The applicability of forecast methods for PVD-assisted staged riprap filling technique can be summarized in Table 4 for short-term and medium-term settlement forecasting, and for long-term and final settlement forecasting, respectively.

Table 4. Applicability of different settlement forecast methods. (SMF—short-term and medium-term settlement forecast; LFF—long-term and final settlement forecast; ○—appropriate; ×—inappropriate.)

Forecast Method	Edge of Berm		Center of Berm		Center of Embankment	
	SMF	LFF	SMF	LFF	SMF	LFF
HM	×	×	×	×	×	×
ECM	×	○	×	○	×	○
PGCM	×	×	○	○	○	○
GGCM	×	×	○	○	○	○
GM	×	○	○	×	×	○
GVM	×	○	○	○	○	○
BPLM	×	×	×	×	×	×
BPGD	○	○	○	○	○	○

For short-term and medium-term settlement forecasts, at the edge of the berm (Point A), only BPGD was available. This might be due to the fact that the settlement at Point A was not only controlled by the staged loading of the berm, but also obviously affected by the subsequent staged loading of the embankment. Therefore, the forecast methods based on a certain curve regulation, for example, EFMs, GCMs, and GPMs, found it difficult to accurately judge the development trend of settlement at this kind of position. However,

the BPGD can feed error rates back through a neural network to make the forecasting more accurate than other methods, and it can solve some shortcomings associated with the BPLM, such as falling into local minimum and the error of artificially choosing the learning rate before training. Moreover, PGCM, GGCM, GM, GVM, and BPGD were available for settlement forecasting at the center of the berm (Point B). In addition, for forecasting at the center of the embankment (Point C), PGCM, GGCM, GVM, and BPGD were available. That is to say, the HM, ECM, and BPLM were not suitable for short-term and medium-term settlement forecasts at all.

For long-term and final settlement forecasts, at the edge of the berm (Point A), ECM, GM, GVM, and BPGD were available. It can be found that the long-term and final settlements at the edge of the berm had a strong exponential regularity. Furthermore, ECM, PGCM, GGCM, GVM, and BPGD were available for Point B at the center of the berm. In addition, at the center of the embankment (Point C), ECM, PGCM, GGCM, GM, GVM, and BPGD were available. It can be observed that, ECM, GVM, and BPGD were appropriate for long-term and final settlement forecasting at all different locations. This is due to the fact that, the ECM and GVM have good exponential characteristics with a saturation region, which can describe the long-term and final settlements of PVD-assisted staged riprap filling foundation in deep marine soft soils well. At the same time, the BPGD was also suitable for long-term and final settlement forecasts at different locations due to its methodological advantages as mentioned above.

By comparing the eight different settlement forecast methods considering the creep of marine soft soils in this case study, the results demonstrated that the applicable conditions of different forecast methods were different, which was mainly due to the different loadings, interaction of foundation soils, and the effect of ground treatment on different foundation positions. Therefore, the settlements at different positions conform to different forms and patterns of variations, and the available forecast methods should be selected according to the specific position and time period. Although these settlement forecast methods have sufficient accuracy, there are still deficiencies in the physical and engineering meanings on forecasting formula and parameters by comparing with analytical calculation and numerical simulation. This will also be a further development direction for the settlement forecast methods in future.

## 5. Conclusions

From the short-term and medium-term, and the long-term and final settlement results that were forecasted by HM, ECM, PGCM, GGCM, GM, GVM, BPLM, and BPGD methods at different locations (such as at the edge of the berm, and at the center of the berm and embankment) of marine soft soil ground under PVD-assisted staged riprap filling technique, the following conclusions for this case study were obtained.

- (1) For different time periods during the settlement process and different locations of marine soft soil foundation, the appropriate and reliable forecast methods were different. Only BPGD was appropriate for settlement forecasting at different time periods and at different locations. This may be due to the fact that the BPANN can feed error rates back through a neural network to make the forecasting more accurate than other methods. Furthermore, the BPGD can solve some shortcomings associated with the BPLM, such as falling into local minimum and the error of artificially choosing the learning rate before training.
- (2) For short-term and medium-term settlement forecasts, the forecast methods can be evaluated by relative errors and evaluation metrics analysis in regression, scilicet when  $0 \geq e > -1\%$ , both the forecasting accuracy and engineering safety are appropriate and reliable. Therefore, for settlement forecasting at the edge of the berm (Point A), only BPGD was available. Moreover, PGCM, GGCM, GM, GVM, and BPGD were available for settlement forecasting at the center of the berm (Point B). In addition, for forecasting at the center of the embankment (Point C), PGCM, GGCM, GVM, and BPGD were available.

- (3) For long-term and final settlement forecasts, at the edge of the berm (Point A), ECM, GM, GVM, and BPGD were available. ECM, PGCM, GGCM, GVM, and BPGD were available for Point B at the center of the berm. Furthermore, at the center of the embankment (Point C), ECM, PGCM, GGCM, GM, GVM, and BPGD were available. In addition to the BPGD, ECM and GVM were also appropriate for long-term and final settlement forecasts at different locations, because they have an exponential shape with a saturation region, which can well describe the long-term and final settlements.
- (4) Since this study was a case study of Lingni Seawall, its applicability needs to be further verified based on more engineering cases in order to form a complete methodology and provide a reference for the selection of forecast models for different ground soils under various hydrogeological conditions. For deep soft soil ground with high water content, high compressibility, and high organic content, the forecast method can be selected by referring to the above results, because these soils have creep characteristics and non-negligible secondary consolidation settlement. However, for silty and sandy soil grounds with low water content and low compressibility, the HM may be not suitable, because the predicted values of HM are too large even for soft clay grounds. On the contrary, for silty and sandy soil grounds, BPLM and GVM may be more suitable due to their smaller predicted values for soft clay grounds.

In addition, although BPGD is the most accurate and feasible model for marine soft soil ground, the process of forecast modeling is complex. Therefore, when it is not necessary to establish a unified forecasting model of full-time and full-project monitoring points to describe the settlement process, a simpler forecast method can be selected for each time period and at each monitoring point based on the above results. Furthermore, it is necessary to find a new forecast method or nonlinear logic algorithm with fewer parameters and stronger applicability for this kind of engineering project.

Nevertheless, the goal of case histories is not only to obtain a splendid best fitting, but also to inverse and calibrate the geotechnical parameters, such as compression coefficient and compression index, especially the secondary compressibility coefficient for compressible marine sediments. More accurate forecasted values could provide a new opportunity for more creditable parameter inversion and calibration. Additionally, it is of great significance to study the mathematical meaning of each parameter in each forecasting model, and more importantly, its physical meaning and the analytical relationship between model parameters and soil geotechnical parameters, which will provide an in-depth understanding of the forecasting algorithm and settlement mechanism.

**Author Contributions:** Conceptualization, X.-T.W. and N.Y.; methodology, X.-T.W., A.A. and N.Y.; software, X.-T.W., J.-N.L. and M.A.; validation, A.A. and R.I.; formal analysis, X.-T.W., J.-N.L. and A.A.; investigation, X.-T.W. and J.-N.L.; data curation, X.-T.W., J.-N.L. and A.A.; writing—original draft preparation, X.-T.W.; writing—review and editing, X.-T.W., A.A., N.Y. and R.I.; visualization, J.-N.L. and M.A.; supervision, N.Y. All authors have read and agreed to the published version of the manuscript.

**Funding:** This research was funded by National Natural Science Foundation of China (Grant Number 52178370 and 41602319), and China Scholarship Council (Grant Number 202006415016).

**Data Availability Statement:** The data presented in this study are available on request from the corresponding author. The data are not publicly available due to ongoing research.

**Acknowledgments:** The authors are indebted to First Highway Consultants Company Limited of China Communications Construction Company and Wenzhou Traffic and Transportation Bureau for their assistance in the field investigation of this project.

**Conflicts of Interest:** The authors declare no conflicts of interest. The funders had no role in the design of the study; in the collection, analyses, or interpretation of data; in the writing of the manuscript, or in the decision to publish the results.

## Abbreviations

The following abbreviations are used in this manuscript:

EFM	Empirical Formula Method
3PM	Three-Point Method
AM	Asaoka Method
HNM	Hoshino Nori Method
HM	Hyperbolic Method
ECM	Exponential Curve Method
GCM	Growth Curve Modeling
WGCM	Weibull Growth Curve Modeling
PGCM	Pearl Growth Curve Modeling
GGCM	Gompertz Growth Curve Modeling
GPM	Grey Prediction Model
GM	Grey (1, 1) Model
GVM	Grey Verhulst Model
ANN	Artificial Neural Network
BP	Back Propagation
BPANN	Back Propagation of Artificial Neural Network
LM	Levenberg–Marquardt
BPLM	BPANN with Levenberg–Marquardt Algorithm
BPGD	BPANN with Gradient Descent of Momentum and Adaptive Learning Rate
PVD	Prefabricated Vertical Drain
SSE	Sum of squares due to error
MSE	Mean squared error
RMSE	Root mean squared error
MAE	Mean absolute error
SMF	Short-term and medium-term settlement forecast
LFF	Long-term and final settlement forecast

## Appendix A

**Table A1.** The monitored time-settlement data-set at Points A, B, and C. ( $t$ —Time;  $S_t$ —Settlement).

Point A		Point B		Point C	
$t$ (d)	$S_t$ (cm)	$t$ (d)	$S_t$ (cm)	$t$ (d)	$S_t$ (cm)
550	108.57	550	140.48	550	223.80
556	108.87	551	140.91	555	225.90
561	108.99	555	141.28	560	228.10
564	109.14	561	141.65	565	230.20
569	109.37	565	142.02	570	232.30
576	109.84	571	142.52	575	234.30
581	110.15	575	143.02	580	236.20
586	110.48	580	143.51	585	238.10
590	110.61	585	143.76	590	239.90
596	111.33	591	144.75	595	241.70
600	111.53	596	145.25	600	243.40
604	111.92	604	146.11	605	244.72
611	112.05	609	146.85	607	245.20
618	112.49	616	147.60	610	245.96
624	112.62	621	147.97	614	247.00
629	112.79	626	148.96	621	248.70
635	112.84	632	149.70	625	249.53
641	113.04	638	150.32	629	250.30
645	113.20	643	150.69	637	251.90
650	113.32	649	150.70	645	253.50
653	113.59	652	151.19	650	254.30
656	113.69	658	151.93	655	255.00

Table A1. Cont.

Point A		Point B		Point C	
<i>t</i> (d)	<i>S<sub>t</sub></i> (cm)	<i>t</i> (d)	<i>S<sub>t</sub></i> (cm)	<i>t</i> (d)	<i>S<sub>t</sub></i> (cm)
659	113.72	661	152.06	660	255.67
665	114.04	665	152.65	665	256.30
673	114.47	668	153.05	670	256.87
678	114.83	674	153.54	675	257.40
685	115.19	678	154.41	680	257.93
691	115.67	683	154.90	685	258.40
697	115.96	687	155.40	690	258.77
705	116.04	692	156.14	695	259.08
709	116.37	695	156.14	697	259.20
713	116.68	699	156.76	700	259.39
717	116.68	704	157.25	705	259.73
723	117.11	709	157.50	709	260.00
726	117.26	715	158.00	715	260.40
730	117.39	720	158.50	720	260.70
733	117.54	726	158.75	725	260.97
736	118.05	731	159.37	730	261.21
738	118.05	736	159.49	732	261.30
740	118.36	742	159.99	740	261.66
745	118.52	745	160.61	745	261.90

## References

- Xia, C.; Deng, Y.; Zhu, M.; Niu, J.; Zheng, L.; Chen, X. One-dimensional solar energy thermal consolidation model testing and analytical calculation for marine soft clays. *J. Mar. Sci. Eng.* **2022**, *10*, 1634.
- Zhou, S.H.; Wang, B.L.; Shan, Y. Review of research on high-speed railway subgrade settlement in soft soil area. *Railw. Eng. Sci.* **2020**, *28*, 129–145.
- Park, H.I.; Kim, K.-S.; Kim, H.Y. Field performance of a genetic algorithm in the settlement prediction of a thick soft clay deposit in the southern part of the Korean peninsula. *Eng. Geol.* **2015**, *196*, 150–157.
- Terzaghi, K. *Erdbaumechanik auf Bodenphysikalischer Grundlage*; Fanz Deuticke: Wien, Austria, 1925.
- Hore, R.; Chakraborty, S.; Ansary, M.A. A field investigation to improve soft soils using prefabricated vertical drain. *Transp. Infrastruct. Geotechnol.* **2020**, *7*, 127–155.
- Cascone, E.; Biondi, G. A case study on soil settlements induced by preloading and vertical drains. *Geotext. Geomembr.* **2013**, *38*, 51–67.
- Prabavathy, S.; Rajagopal, K.; Pitchumani, N. Investigation of smear zone around PVD mandrel using image-based analysis. *Int. J. Geosynth. Ground Eng.* **2021**, *7*, 94.
- Deng, Y.-B.; Liu, G.-B.; Lu, M.-M.; Xie, K.-H. Consolidation behavior of soft deposits considering the variation of prefabricated vertical drain discharge capacity. *Comput. Geotech.* **2014**, *62*, 310–316.
- Skempton, A.W.; Peck, R.B.; MacDonald, D.H. Settlement analyses of six structures in Chicago and London. *Proc. Inst. Civ. Eng.* **1955**, *4*, 525–542.
- Wang, H.; She, H.; Xu, J.; Liang, L. A three-point hyperbolic combination model for the settlement prediction of subgrade filled with construction and demolition waste. *Materials* **2020**, *13*, 1959.
- Parsa-Pajouh, A.; Fatahi, B.; Vincent, P.; Khabbaz, H. Trial embankment analysis to predict smear zone characteristics induced by prefabricated vertical drain installation. *Geotech. Geol. Eng.* **2014**, *32*, 1187–1210.
- Chai, J.C.; Miura, N. Investigation of factors affecting vertical drain behavior. *J. Geotech. Geoenviron. Eng.* **1999**, *125*, 216–226.
- Lin, S.; Fu, D.; Zhou, Z.; Yan, Y.; Yan, S. Numerical investigation to the effect of suction-induced seepage on the settlement in the underwater vacuum preloading with prefabricated vertical drains. *J. Mar. Sci. Eng.* **2021**, *9*, 797.
- Maleki, M.; Alielahi, H.; Rahmani, I. Effect of smear zone characteristics on PVD-improved soft soils using field data and numerical simulations. *Indian Geotech. J.* **2022**, *52*, 1391–1409.
- Muhammed, J.J.; Jayawickrama, P.W.; Teferra, A.; Özer, M.A. Settlement of a railway embankment on PVD-improved Karakore soft alluvial soil. *Eng. Sci. Technol. Int. J.* **2020**, *23*, 1015–1027.
- Zhang, C.; Li, J.; He, Y. Application of optimized grey discrete Verhulst-BP neural network model in settlement prediction of foundation pit. *Environ. Earth Sci.* **2019**, *78*, 441.
- Zeng, G.X.; Yang, X.L. Settlement analysis of sand-drained ground. *J. Zhejiang Univ.* **1959**, *3*, 34–72.
- Asaoka, A. Observational procedure of settlement prediction. *Soils Found.* **1978**, *18*, 87–101.
- Lee, D.-W.; Lim, S.-H. Final settlement prediction methods of embankments on soft clay. *Mag. Korean Soc. Agric. Eng.* **2000**, *42*, 68–77.

20. Tan, T.-S.; Inoue, T.; Lee, S.-L. Hyperbolic method for consolidation analysis. *J. Geotech. Eng.* **1991**, *117*, 1723–1737.
21. Ma, H.; Peng, C.; Gan, J.; Deng, Y. An optimization algorithm for exponential curve model of single pile bearing capacity. *Geotech. Geol. Eng.* **2021**, *39*, 3265–3269.
22. Feng, S.; Lei, H.; Lin, C. Analysis of ground deformation development and settlement prediction by air-boosted vacuum preloading. *J. Rock Mech. Geotech. Eng.* **2022**, *14*, 272–288.
23. Tang, X.; Wang, J. A new combination forecasting method of adaptive fuzzy variable weight. *J. Univ. Electron. Sci. Technol. Algorithm* **1997**, *26*, 289–291.
24. Wang, B.; Wang, X.; Ma, X. Study on optimal combination settlement prediction model based on logistic curve and Gompertz curve. *Civ. Eng. J.* **2020**, *29*, 347–357.
25. Cheng, F.; Zhang, Y.; Wan, Y.; Wang, H. Subsidence prediction of deep foundation pit surrounding surface based on Gompertz model. *J. Undergr. Space Eng.* **2013**, *9*, 541–546.
26. Deng, J.-L. Control problems of grey systems. *Syst. Control. Lett.* **1982**, *1*, 288–294.
27. Wan, K.; Li, B.; Zhou, W.; Zhu, H.; Ding, S. A novel time-power based grey model for nonlinear time series forecasting. *Eng. Appl. Artif. Intell.* **2021**, *105*, 104441.
28. Kayacan, E.; Ulutas, B.; Kaynak, O. Grey system theory-based models in time series prediction. *Expert Syst. Appl.* **2010**, *37*, 1784–1789.
29. Huang, C.; Zhou, L.; Liu, F.; Cao, Y.; Liu, Z.; Xue, Y. Deformation prediction of dam based on optimized Grey Verhulst Model. *Mathematics* **2023**, *11*, 1729.
30. Ebid, A.M. 35 Years of (AI) in geotechnical engineering: State of the art. *Geotech. Geol. Eng.* **2021**, *39*, 637–690.
31. Raja, M.N.A.; Shukla, S.K. Predicting the settlement of geosynthetic-reinforced soil foundations using evolutionary artificial intelligence technique. *Geotext. Geomembr.* **2021**, *49*, 1280–1293.
32. Ye, X.-W.; Jin, T.; Chen, Y.-M. Machine learning-based forecasting of soil settlement induced by shield tunneling construction. *Tunn. Undergr. Space Technol.* **2022**, *124*, 104452.
33. Wang, Z.-L.; Li, Y.-C.; Shen, R. Correction of soil parameters in calculation of embankment settlement using a BP network back-analysis model. *Eng. Geol.* **2007**, *91*, 168–177.
34. Levenberg, K. A method for the solution of certain non-linear problems in least squares. *Q. Appl. Math.* **1944**, *2*, 164–168.
35. Marquardt, D.W. An algorithm for least-squares estimation of nonlinear parameters. *J. Soc. Ind. Appl. Math.* **1963**, *11*, 431–441.
36. Wang, Z.L.; Li, X.Y.; Yin, Z.Z. Application of genetic and improved BP algorithms in geotechnical engineering. *Undergr. Space* **2001**, *21*, 15–17.
37. Pham, Q.D.; Ngo, V.L.; Trinh, M.T. Evaluation of Asaoka and Hyperbolic methods for settlement prediction of vacuum preloading combined with prefabricated vertical drains in soft ground treatment. *J. Eng. Technol. Sci.* **2022**, *54*, 859.
38. Liu, J.; Yang, Y.; Yang, C. Analysis and prediction of long-term settlement of metro shield tunnel in saturated sand. *Geotech. Geol. Eng.* **2021**, *39*, 5241–5252.
39. Ebid, A.M.; Onyelowe, K.C.; Salah, M.; Adah, E.I. Using FEM-AI technique to predict the behavior of strip footing rested on undrained clay layer improved with replacement and geo-grid. *Civ. Eng. J.* **2023**, *9*, 1230–1243.
40. Muhammed, J.J.; Jayawickrama, P.W.; Ekwaro-Osire, S. Uncertainty analysis in prediction of settlements for spatial prefabricated vertical drains improved soft soil sites. *Geosciences* **2020**, *10*, 42.
41. Mishra, S.K. *Riprap Design for Overtopped Embankments*; Colorado State University: Fort Collins, CO, USA, 1998.
42. Mei, G.X.; Zai, J.M.; Zhao, W.B.; Yin, J.H. Settlement prediction methods considering creep. *Chin. J. Geotech. Eng.* **2004**, *26*, 416–418.
43. Wang, Z.L.; Huang, J.Z.; Yang, X.H. Study on settlement prediction model considering rheological properties of soils. *Rock Soil Mech.* **2006**, *27*, 1567–1570.
44. Gao, Z.X.; Sun, X. Research on predicting model and method of final settlement of rheological soft soil subgrade. *Site Investig. Sci. Technol.* **2008**, *26*, 3–6.
45. Kang, H.; Peng, Z.B. Research and analysis of forecast model for settlement of soft soil foundation. *Min. Metall. Eng.* **2009**, *29*, 9–11.
46. Kong, X.X. Research and application on the prediction method of Pearl model of high filling subgrade settlement. In *Proceedings of the Soil Testing, Soil Stability and Ground Improvement: Proceedings of the 1st GeoMEast International Congress and Exhibition*; Springer: Cham, Switzerland, 2018; pp. 356–362.
47. Hou, H.; Andrews, H. Cubic splines for image interpolation and digital filtering. *IEEE Trans. Acoust. Speech Signal Process.* **1978**, *26*, 508–517.
48. Wu, X.-T. Research on relation between consolidation coefficient and consolidation stress of silt in Wenzhou shoal. *Rock Soil Mech.* **2013**, *34*, 1675–1680.
49. Wu, X.-T.; Liu, J.-N.; Xie, Z.-M. Deformation and strength characteristics of marine soft soil treated by Prefabricated Vertical Drain-assisted staged riprap under seawall construction. *Buildings* **2023**, *13*, 2322.
50. Fan, H.; Chen, Z.; Shen, J.; Cheng, J.; Chen, D.; Jiao, P. Buckling of steel tanks under measured settlement based on Poisson curve prediction model. *Thin-Walled Struct.* **2016**, *106*, 284–293.
51. Tan, S.; Chew, S. Comparison of the hyperbolic and Asaoka observational method of monitoring consolidation with vertical drains. *Soils Found.* **1996**, *36*, 31–42.
52. Pan, L.-Y.; Xie, X.-Y. Observational settlement prediction by curves fitting methods. *Rock Soil Mech.* **2004**, *25*, 1053–1058.
53. Li, G.H.; Liu, H.B.; Qin, X.X. Settlement prediction of roadbed based on mixture model with exponential curve and ANN. *Adv. Mater. Res.* **2013**, *663*, 76–79.

54. Ishibashi, I.; Hazarika, H. *Soil Mechanics Fundamentals and Applications*; CRC Press: Boca Raton, FL, USA, 2015.
55. Zhao, M.H.; Long, Z.; Zou, X.J. Optimal combinational predictive model of settlement based on Logistic curve and Gompertz curve and its application. *J. Highw. Transp. Res. Dev.* **2007**, *24*, 1–4.
56. Deng, J.L. Introduction to grey system theory. *J. Grey Syst.* **1989**, *1*, 1–24.
57. Wang, Z.-X.; Dang, Y.-G.; Liu, S.-F. Unbiased grey Verhulst model and its application. *Syst. Eng.-Theory Pract.* **2009**, *29*, 138–144.
58. Han, L. *Artificial Neural Network Theory, Design and Application*; Chemical Industry Publishing House: Beijing, China, 2007.
59. Tanabashi, Y.; Mawatari, T.; Gotoh, K.; Yasuhara, K.; Kouno, H. On the applicability of some settlement prediction methods to the soft Ariake clay ground. *Rep. Fac. Eng. Nagasaki Univ.* **1994**, *24*, 241–248.
60. Xu, X.X.; Su, H.Y.; Zhang, C.P. Application of BP neural network to short-term prediction foundation settlement in the base pit vicinity. *J. Sichuan Univ. Sci. Eng. (Nat. Sci. Ed.)* **2013**, *26*, 53–56.
61. Lei, H.Y.; Wan, Y.F.; Feng, S.X. Study on long-term settlement law and prediction of deep beach soft soil subgrade under different tidal levels. *J. Tianjin Univ. (Sci. Technol.)* **2022**, *55*, 584–595.

**Disclaimer/Publisher’s Note:** The statements, opinions and data contained in all publications are solely those of the individual author(s) and contributor(s) and not of MDPI and/or the editor(s). MDPI and/or the editor(s) disclaim responsibility for any injury to people or property resulting from any ideas, methods, instructions or products referred to in the content.